

# Multiplex coherent anti-Stokes Raman scattering (MCARS) for chemically sensitive, label-free flow cytometry

Charles H. Camp Jr.<sup>1\*</sup>, Siva Yegnanarayanan<sup>1</sup>, Ali A. Eftekhar<sup>1</sup>,  
Hamsa Sridhar<sup>2</sup>, and Ali Adibi<sup>1</sup>

<sup>1</sup>*School of Electrical and Computer Engineering, Georgia Institute of Technology,  
777 Atlantic Dr., Atlanta, GA, 30332*

<sup>2</sup>*Current Address: Harvard University, Cambridge, MA, 02138*

[ccampjr@ece.gatech.edu](mailto:ccampjr@ece.gatech.edu)

**Abstract:** Flow cytometry is an ever-advancing high-throughput multivariate analysis tool that natively provides size and morphological information. To obtain molecular information, however, typically requires the addition of fluorophores, which are limited by spectral overlap, non-specific binding, available conjugation chemistries, and cellular toxicity. A complementary or alternative, label-free approach to molecular information is through multiplex coherent anti-Stokes Raman scattering (MCARS), which is a coherent, nonlinear optical method that provides a wealth of molecular information by probing the Raman energies within a molecule. In this work, we demonstrate the unique capability of our MCARS flow cytometer to distinguish flowing particles and discuss system performance capabilities and possibilities.

© 2009 Optical Society of America

**OCIS codes:** (190.4380) Nonlinear optics, four-wave mixing; (190.7110) Ultrafast nonlinear optics; (300.6230) Spectroscopy, coherent anti-Stokes Raman scattering.

---

## References and links

1. W. H. Coulter, "High speed automatic blood cell counter and analyzer," in *Proceedings of the National Electronics Conference*, **12**, 1034-1040 (1956).
2. H. M. Shapiro, *Practical Flow Cytometry*, 4th ed. (Wiley Liss, New York, 2003).
3. M. G. Macey, "Principles of flow cytometry," in *Flow Cytometry: Principles and Applications*, M. G. Macey, ed. (Humana, Totowa, New Jersey, 2007), pp. 1-15.
4. N. Baumgarth and M. Roederer, "A practical approach to multicolor flow cytometry for immunophenotyping," *J. Immunological Methods* **243**, 77-97 (2000).
5. D. A. McCarthy, "Fluorochromes and fluorescence," in *Flow Cytometry: Principles and Applications*, M. G. Macey, ed. (Humana, Totowa, New Jersey, 2007), pp. 59-112.
6. Z. Darzynkiewicz, M. Roederer, and H. J. Tanke, eds., *Cytometry, 4<sup>th</sup> Edition: New Developments*, 4th ed., **75**, (Elsevier Academic, San Diego, Calif., 2004).
7. A. D. Michelson, "Flow cytometry: a clinical test of platelet function," *Blood* **87**, 4925-4936 (1996).
8. M. Roederer, "Spectral Compensation for Flow Cytometry: Visualization Artifacts, Limitations, and Caveats," *Cytometry* **45**, 194-205 (2001).
9. G. Goddard, J. C. Martin, M. Naivar, P. M. Goodwin, S. W. Graves, R. Habbersett, J. P. Nolan, and J. H. Jett, "Single particle high resolution spectral analysis flow cytometry," *Cytometry Part A* **69A**, 842-851 (2006).
10. D. A. Watson, L. O. Brown, D. F. Gaskill, M. Naivar, S. W. Graves, S. K. Doorn, and J. P. Nolan, "A flow cytometer for the measurement of Raman spectra," *Cytometry Part A* **73A**, 119-128 (2008).
11. A. Y. Lau, L. P. Leeb, and J. W. Chan, "An integrated optofluidic platform for Raman-activated cell sorting," *Lab on a chip* **8**, 1116-1120 (2008).

12. J. W. Chan, D. S. Taylor, T. Zwerdling, S. M. Lane, K. Ihara, and T. Huser, "Micro-Raman spectroscopy detects individual neoplastic and normal hematopoietic cells," *Biophys. J.* **90**, 648-656 (2006).
13. J. X. Cheng, A. Volkmer, and X. S. Xie, "Theoretical and experimental characterization of coherent anti-Stokes Raman scattering microscopy," *J. Opt. Soc. Am. B* **19**, 1363-1375 (2002).
14. C. L. Evans and X. S. Xie, "Coherent anti-Stokes Raman scattering microscopy: chemical imaging for biology and medicine," *Annu. Rev. Anal. Chem.* **1**, 883-909 (2008).
15. H. Kano and H. Hamaguchi, "Vibrationally resonant imaging of a single living cell by supercontinuum-based multiplex coherent anti-Stokes Raman scattering microspectroscopy," *Opt. Express* **13**, 1322-1327 (2005).
16. H. A. Rinia, M. Bonn, E. M. Vartiainen, C. B. Schaffer, and M. Müller, "Spectroscopic analysis of the oxygenation state of hemoglobin using coherent anti-Stokes Raman scattering," *J. Biomed. Opt.* **11**, 050502(2006).
17. C. L. Evans, E. O. Potma, M. Puorishaag, D. Cote, C. P. Lin, and X. S. Xie, "Chemical imaging of tissue in vivo with video-rate coherent anti-Stokes Raman scattering microscopy," *PNAS* **102**, 16807-16812 (2005).
18. J. X. Cheng, A. Volkmer, L. D. Book, and X. S. Xie, "An Epi-Detected Coherent Anti-Stokes Raman Scattering (E-CARS) Microscope with High Spectral Resolution and High Sensitivity," *J. Phys. Chem. B* **105**, 1277-1280 (2001).
19. H. Kano, "Molecular vibrational imaging of a human cell by multiplex coherent anti-Stokes Raman scattering microspectroscopy using a supercontinuum light source," *J. Raman Spectrosc.* **39**, 1649-1652 (2008).
20. H. W. Wang, N. Bao, T. T. Le, C. Lu, and J. X. Cheng, "Microfluidic CARS cytometry," *Opt. Express* **16**, 5782-5789 (2008).
21. M. Müller and J. M. Schins, "Imaging the Thermodynamic State of Lipid Membranes with Multiplex CARS Microscopy," *J. Phys. Chem. B*, **106**, 3715-3723 (2002).
22. G. W. H. Wurpel, J. M. Schins, and M. Müller, "Chemical specificity in three-dimensional imaging with multiplex coherent anti-Stokes Raman scattering microscopy," *Opt. Lett.* **27**, 1093-1095 (2002).
23. J. X. Cheng, A. Volkmer, L. D. Book, and X. S. Xie, "Multiplex Coherent Anti-Stokes Raman Scattering Microspectroscopy and Study of Lipid Vesicles," *J. Phys. Chem. B* **106**, 8493-8498 (2002).
24. H. N. Paulsen, K. M. Hilligsøe, J. Thøgersen, S. R. Keiding, J. J. Larsen, "Coherent anti-Stokes Raman scattering microscopy with a photonic crystal fiber based light source," *Opt. Lett.*, **28**, 1123-1125 (2003).
25. K. P. Knutsen, J. C. Johnson, A. E. Miller, P. B. Petersen, R. J. Saykally, "High spectral resolution multiplex CARS spectroscopy using chirped pulses," *Chem. Phys. Lett.* **387**, 436-441 (2004).
26. E. R. Andresen, H. N. Paulsen, V. Birkedal, J. Thøgersen, and S. R. Keiding, "Broadband multiplex coherent anti-Stokes Raman scattering microscopy employing photonic-crystal fibers," *J. Opt. Soc. Am. B* **22** 1934-1938 (2005).
27. D. Schafer, J. A. Squier, J. van Maarseveen, D. Bonn, M. Bonn, and M. Müller, "In situ quantitative measurement of concentration profiles in a microreactor with submicron resolution using multiplex CARS microscopy," *J. Am. Chem. Soc.* **130**, 11592-11593 (2008).
28. J. Herrmann, U. Griebner, N. Zhavoronkov, A. Husakou, D. Nickel, J. C. Knight, W. J. Wadsworth, P. St. J. Russell, and G. Korn, "Experimental evidence for supercontinuum generation by fission of higher-order solitons in photonic fibers," *Phys. Rev. Lett.* **88**, 173901 (2002).
29. G. P. Agrawal, *Nonlinear Fiber Optics*, 3rd ed. (Academic, San Diego, Calif., 2001).
30. C. H. Camp Jr., A. A. Eftekhar, and A. Adibi, "Single-source interferometric multiplex coherent anti-Stokes Raman scattering with a photonic crystal fiber light source," Conference on Lasers and Electro-Optics (CLEO), San Jose, CA, May 4-9, 2008.
31. T. M. Squires and S. R. Quake, "Microfluidics: fluid physics at the nanoliter scale," *Rev. Mod. Phys.* **77**, 977-1026 (2005).
32. G. M. Whitesides, "The origins and the future of microfluidics," *Nature* **442**, 368-373 (2006).
33. R. M. Waxler, D. Horowitz, and A. Feldman, "Optical and physical parameters of Plexiglas 55 and Lexan," *Appl. Opt.* **18**, 101-104 (1979).
34. X. Ma, J. Q. Lu, R. S. Brock, K. M. Jacobs, P. Yang, and X. H. Hu, "Determination of complex refractive index of polystyrene microspheres from 370 to 1610 nm," *Phys. Med. Biol.* **48**, 4165-4172 (2003).
35. M. L. Shuler, R. Aris, and H. M. Tsuchiya, "Hydrodynamic focusing and electronic cell-sizing techniques," *Appl. Microbiol.*, **24**, 384-388 (1972).
36. K. Pearson, "On lines and planes of closest fit to systems of points in space," *Philosophical Magazine* **2**, 559-572 (1901).
37. J. X. Cheng and X. S. Xie, "Coherent Anti-Stokes Raman Scattering Microscopy: Instrumentation, Theory, and Applications," *J. Phys. Chem. B* **108**, 827-840 (2004).
38. Newport Corporation, "Oriel InstaSpec X CCD," <http://www.newport.com/store/genproduct.aspx?id=415018>.
39. Andor Technology plc, "Andor Newton 970 EMCCD Camera," [http://www.andor.com/scientific\\$\\_cameras/newton/models/default.aspx?ProductCodeID=48](http://www.andor.com/scientific$_cameras/newton/models/default.aspx?ProductCodeID=48).
40. Princeton Instruments, "PIXIS - CCD (spectroscopy Version)," <http://www.princetoninstruments.com/products/speccam/pixis/>.

41. J. W. Bales, "Ultra-high-speed imaging: High-speed and ultra-high-speed imaging offers broad application coverage," *Laser Focus World*, <http://www.laserfocusworld.com/articles/282677>.
  42. Cordin Scientific Imaging, "Rotating mirror cameras," <http://www.cordin.com/productsrm.html>.
  43. Massachusetts Institute of Technology, "The Edgerton Center: High Speed Imaging Links," <http://web.mit.edu/Edgerton/www/HSILinks.html>.
- 

## 1. Introduction

Over the last half-century, flow cytometry has evolved from its modest roots as a cell counter/sizer that measured impedance changes as particles flowed past, to complex multivariate systems that use optics and electronics to measure an ever-growing variety of phenotypes. Information about size and morphology is traditionally gathered from analyzing photons elastically scattered off of passing particles or electrically measuring impedance changes across a target area of the flow volume [1–3]. To ascertain molecular information, however, typically requires the addition of fluorescent labels [2–6]. These labels, although a powerful tool, have limitations and challenges such as large emission spectra, nonspecific binding, available conjugation chemistries, and cytotoxicity, which can alter cellular chemistries and perturb the experimental outcomes [2,4]. Additionally, the process of conjugating fluorophores and labeling cells can be time consuming; thus, reducing clinical turn-around times and affecting time-sensitive samples (e.g. [7]).

In the last 10 years, flow cytometry has increasingly pushed the boundaries of the number of simultaneously measurable colors and in doing so realized analyses not possible or probable with fewer colors [4]. As the amount of information scales geometrically with the number of color channels, there is a continued push for more channels and more information. This expansion, however, has increased the complexities of selecting and utilizing fluorophores and increased the demands on system of system optics and detectors. One of the largest challenges facing multicolor systems is from the spectral overlap between color channels resulting from the broadband emission spectra of the individual fluorophores. Although one could subdivide a sample and separately label and analyze the aliquots, this is not always practical when sample volumes are limited such as with pediatric samples or when analyzing rare cells [4]. Another option that cytometer vendors and independent researchers have actively engaged, is the use of compensation methods, which are mathematical models designed to reduce the effects of spectral bleed. Although these methods applied in hardware and software can be effective, they bring along their own complications, limitations, and errors [4, 8]. Alternatively, the use of detector arrays to capture the full fluorescence spectrum was developed and demonstrated the capability to detect multiple fluorophore-labeled samples with a good degree of accuracy [9].

To circumvent these problems, several groups have used Raman scattering based methods to probe the chemically specific vibrational levels of passing samples [10, 11]. These vibrational levels provide rich information about the state of the molecule and provide a mechanism for differentiating samples in a label-free manner. Chan *et al.*, for example, demonstrated the vibrational differences of healthy and neoplastic lymphocytes [12]. These methods can be used in conjunction with fluorescent techniques, or possibly in some instances, to replace them entirely. Raman scattering, however, is a relatively weak process; thus, requiring techniques such as surface enhancement with nanoparticles [10] to be feasible for high throughput systems (HTS). Related, coherent techniques also probe the Raman vibrational levels within molecules, but with much higher efficiencies. One such method, which has shown promise in analyzing biological samples, is coherent anti-Stokes Raman scattering (CARS) [13, 14].

CARS is a third-order nonlinear process in which two photons (pump and Stokes) excite a vibrational (Raman) transition, and a third photon (probe) inelastically scatters off of the excited sample. As compared to traditional Raman spectroscopies, CARS is a coherent pro-

cess, which leads to much higher process efficiency; thus, the CARS signal can be several orders of magnitude larger than spontaneous Raman. Additionally, CARS is a parametric process that generates blue-shifted, anti-Stokes photon; therefore, there is no spectral overlap with sample fluorescence, which can obscure or completely hide the conventional Raman signal. These strengths have evolved CARS microscopy into an advanced imaging and spectroscopic modality that has been successfully applied to a number of biologically relevant samples, for example: yeast cells [15], oxy-/deoxyhemoglobin [16], live animal cells [17], and unstained human cells [13, 14, 18, 19]. Recently, CARS has been applied toward microfluidic flow cytometry [20]. In this implementation of CARS, the relative energy (frequency) between the pump and the Stokes sources was tuned to selectively excite a single Raman vibration; therefore, providing vibrationally selective flow cytometry.

In this work, we demonstrate a label-free microfluidic flow cytometer based on multiplex CARS (MCARS), which excites multiple transitions simultaneously; thus, providing a more complete vibrational picture than found with vibrationally selective techniques (such as CARS) [21–26]. Additionally, this broadband technology provides a similar wealth of information as conventional Raman spectroscopy, but at emission intensities large enough for high-speed detection; thus, opening up the possibility of integration with current flow cytometers that can work in excess of 10,000 particles per second. Recently, the molecular sensitivity of MCARS was applied to microfluidics in order to measure the concentration profiles of mixing species within a microreactor with unprecedented sensitivity [27]. In this work, we extend this method's sensitive, multispectral abilities to the dynamic situation of characterizing flowing particles. To demonstrate this molecular sensitivity, we analyze a sample composed of polymer beads of the same size but differing composition (polystyrene and poly(methyl methacrylate)). Looking at the spectral content of the passing samples, allowed for clear distinction between the different beads (and the aqueous surroundings). Additionally, we analyze the performance of our particular system, and discuss the optimal-yet-feasible performance of the technology.

## 2. Experimental apparatuses, materials, and techniques

### 2.1. MCARS Spectrometer

Coherent anti-Stokes Raman scattering (CARS) is a nonlinear optical process that probes the vibrational levels within a material; thus, providing molecularly specific information. Two photons, pump and “Stokes”, excite the material into a higher vibrational level, and a probe photon inelastically scatters off [see Fig. 1(a)]. In this implementation, the energy difference between the pump, Stokes, and probe are tuned to correspond to Raman energy levels. Multiplex CARS, however, uses a broadband Stokes (or pump) source to excite multiple Raman transitions simultaneously [see Fig. 1(b)] [21–26]. As shown in Fig. 2(a), our system uses a sub-150 fs source (MIRA, Coherent, Santa Clara, CA) to act as both pump (degenerate probe) and seed source for a length of photonic crystal fiber (PCF) (FemtoWhite 800, NKT Photonics A/S, Birkerød, Denmark) [24, 26]. Within the PCF, an interplay of linear and nonlinear effects; such as soliton formation, decay, and collapse; produces a supercontinuum [28, 29] that is used as the broadband Stokes source. The raw spectrum from the PCF is long-pass filtered to remove wavelengths below the 806 nm pump, which would act only to interfere with the anti-Stokes signal [30]. The excitation sources are coupled into an inverted, customized microscope (BXFM, Olympus, Tokyo, Japan) and focused on the sample with a 100x oil-immersion objective (Planachromatic Micromaster, Fisher Scientific, Pittsburgh, PA) providing a focal volume less than 500 nm across and approximately 1.5  $\mu\text{m}$  axially. The MCARS spectrum is collected in the forward direction with a 10x long-working distance objective (LMPlanFI, Olympus, Tokyo, Japan) into the collimator tip of a fiber-coupled, charge-coupled device (CCD) spectrometer (InstaSpecX, Newport Stratford, Inc., Stratford, CT), recorded in LabVIEW and analyzed in MATLAB.

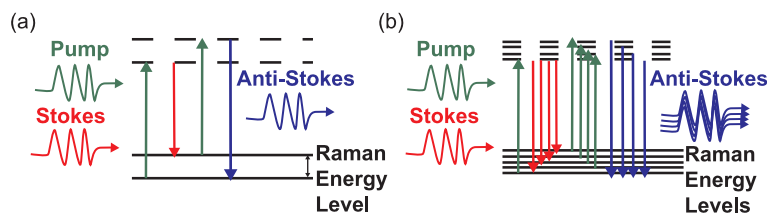


Fig. 1. (Color online) Energy level diagrams of CARS (a) and MCARS (b).

## 2.2. Microfluidics

Microfluidic devices, due to their small feature size, provide high sensitivity while using sample and analyte volumes into the nano- and picoliter range [31, 32]. To provide a confined and controllable area in which to flow our sample, we used a commercially available glass chip (X3550, Micronit Microfluidics BV, Netherlands) with a cross architecture [see Fig. 2(b)]. The cross architecture, with 3 inputs and 1 output, allows for independent sheath and sample flows that provide a hydrodynamic method for sample confinement. The channels are  $20\ \mu\text{m}$  deep and  $60\ \mu\text{m}$  wide. The chip is coupled to a syringe pump (PHD 2000, Harvard Apparatus, Holliston, MA) with polymer ports and adapters (NanoPorts, IDEX Health and Science, Oak Harbor, WA) that provides an air-tight seal with low dead volume for up to 1500 psi, which supports aqueous flows up to approximately  $75\ \mu\text{L}/\text{min}$ .

## 2.3. Sample preparation and administration

To demonstrate the molecular sensitivity of our MCARS flow cytometer, we selected  $5\ \mu\text{m}$  spheres of polystyrene (PS) (Thermo Scientific, Waltham, MA) and poly(methyl methacrylate) (PMMA) (Phosphorex, Fall River, MA). These spheres, with indexes of refraction of 1.49 for PMMA [33] and 1.58 for PS [34], are (linearly) optically similar, but have distinctly different CARS spectra (see Fig. 3). Each type of microsphere solution was mixed in an approximately 1 : 1 ratio and added to 2% detergent solution composed of Tween 20 (Promega, Madison, WI) and deionized water to prevent aggregation, which may hamper smooth flow or clog the channel entirely. The final sample concentration was approximately 2% solids and 98% liquid; although, particle aggregation at the sample inlets changed the measured ratios in most experiments to approximately 50% solids.

In order to administer the samples, we needed a method to ensure orderly, single particle flow through the optical focal region. The traditional method of sample confinement in flow cytometry, hydrodynamic focusing, encapsulates the sample flow with a high-speed sheath flow [35]. As long as the sheath fluids vary in viscosity or velocity from the sample, the flows do not mix, and the sample flow is relatively well contained. In many flow cytometers, the focal volume is an ellipsoid that is wider than the sample flow; thus, it is able to accurately capture particle sizes while remaining relatively insensitive to the exact spatial location of the particle within the sample flow. As CARS is a third-order nonlinear optical process, spreading the incident beam over a large area (relative to the particle sizes) would dramatically reduce the number of anti-Stokes photons generated; thus, it is an impractical approach for covering the entire area of the sample flow. A simple alternative that we conceived of is “hydrodynamic herding”, where particles flow along the channel side-walls in an effort to fix the transverse location of all flowing particles (see Fig. 4). For this work, we used a  $100\ \mu\text{L}$  syringe (lateral port) and a

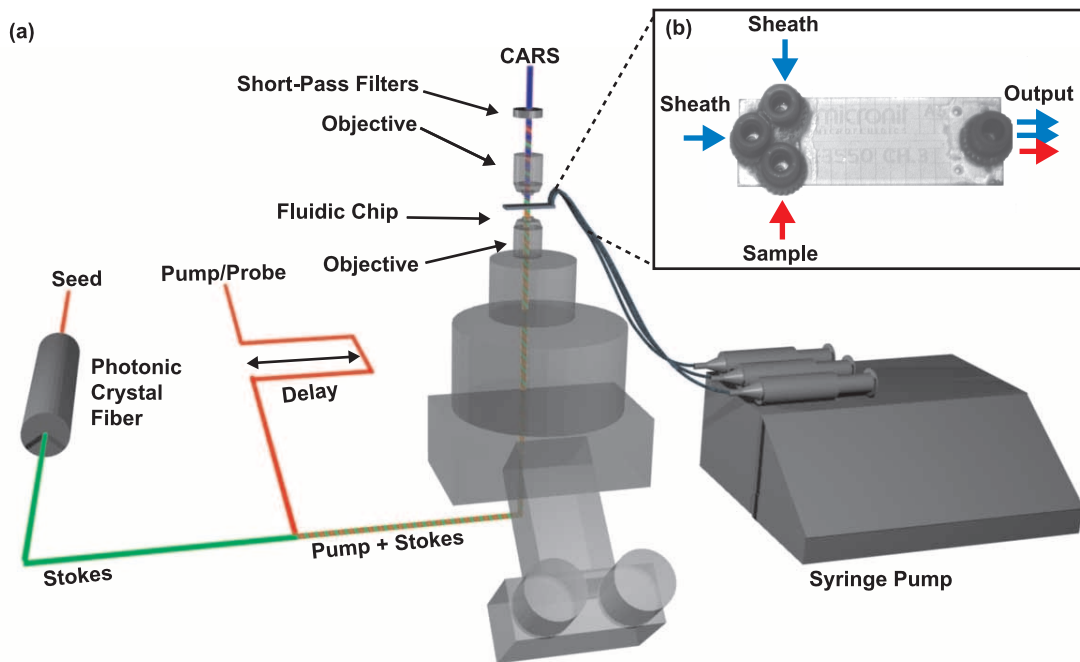


Fig. 2. (Color online) (a) Schematic of the MCARS microfluidic flow cytometer. The ultrafast source acts as both the CARS excitation pulse and a seed for a length of photonic crystal fiber, which is spectrally filtered and recombined with the pump (temporally and spatially overlapped). These sources are focused on the sample with an inverted microscope, and the emitted anti-Stokes signal is collected into a CCD-equipped spectrometer. (b) Image of the microfluidic chip, which has channel widths of  $60\ \mu\text{m}$  and depths of  $20\ \mu\text{m}$ . Each port of the chip is connected to a different size syringe that was selected to provide consistent hydrodynamic herding, in which sample particles are forced to flow against a side wall.

1 mL syringe (axial port) to apply the sheath flow and used the sample port as a reservoir. A negative pressure was applied to the output port with a  $50\ \mu\text{L}$  syringe in order to pull the sample through. We found that this configuration allowed consistent hydrodynamic herding even at low flow rates.

### 3. Experimental results

To demonstrate the molecular sensitivity of our system, we flowed a mixture of PS and PMMA beads in a detergent solution at approximately  $185\ \mu\text{m/s}$  (as measured along the sidewall), which is  $\sim 360\ \text{pL/min}$  at the sample inlet. These beads, although the same size and optically similar, have distinct CARS spectra, and thus are easy to differentiate using our system. Figure 5(a) shows a typical time-stack that captures the MCARS spectra of PS, PMMA, and the broad non-resonant background of water. Individual spectra (smoothed with a 7<sup>th</sup>-order Savitzky-Golay filter) of PMMA and PS are shown in Fig. 5(b) and 5(c), respectively. For this

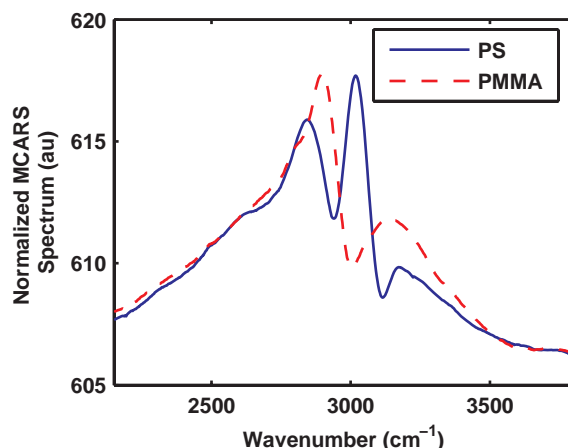


Fig. 3. (Color online) CARS spectra of PS and PMMA measured with our MCARS spectrometer. Although PS and PMMA are optically similar polymers, they show distinct spectral CARS features.

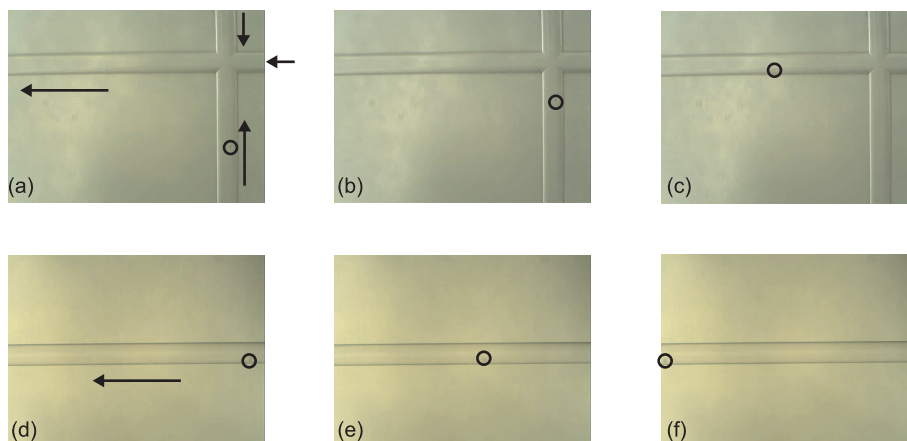


Fig. 4. (Color online) Using hydrodynamic herding, a sample polystyrene bead is forced against a side-wall. Video stills (a)-(c) show the progression of a single bead from the sample inlet (see [Media 1](#)). Frames (d)-(f) show the single bead still against the side and propagating 2 cm away from the cross junction (see [Media 2](#)).

experiment the pump and Stokes source powers were approximately 38 and 8 mW, respectively, and the integration time was approximately  $100 \mu\text{s}$  with full-vertical binning. The particle spectra have a signal-to-noise (SNR) ratio of approximately 14-16 dB. With this integration time and the additional data transfer time, each particle was captured by approximately 3 spectra. Even with this level of signal, the integration time could be significantly reduced (assuming the CCD hardware allows for this) while maintaining the signal necessary to distinguish the particles.

To classify the samples, we used a principle component analysis (PCA) tool developed in MATLAB. PCA is a multivariate analysis tool that reduces the number of variables (in this case, wavelengths) in a given data set by combining them into “principle components” that represent the most prevalent spectral variations [36]. Using this tool, we can classify spectra as PS,

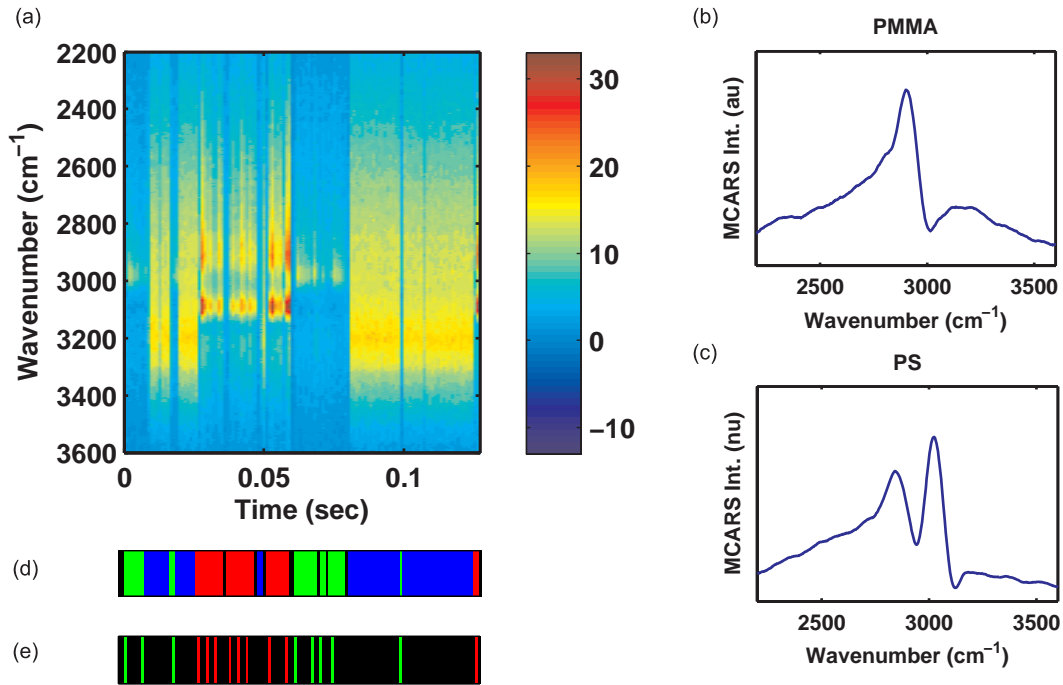


Fig. 5. (Color online) (a) Time-stack MCARS spectra of polystyrene and PMMA beads flowing at approximately  $185 \mu\text{m/s}$ . The total data collection was carried out over 120 ms and the pump and Stokes source powers were approximately 38 and 8 mW, respectively. Example MCARS spectrum of (b) PMMA and (c) PS taken from this time-stack, respectively. (d) Classification of spectra using PCA: green = PMMA, red = PS, blue = water, black = signal below minimum. (e) Particle centers determined by local maxima of spectral intensities

PMMA, water, and other with or without the use of training data sets (in this work, no training sets were used). Figure 5(d) shows this classification of the time-stack in Fig. 5(a), where green is PMMA, red is PS, blue is water, and black is for spectra not significantly above the dark current (usually occurs at the edge of particles due to refraction of the incident beams). This analysis tool was able to distinguish and classify water, PS, and PMMA with 100% accuracy during a large evaluation test set; although, this perfect accuracy would undoubtedly be tested for more complicated and weaker spectra. Each particle is approximately captured by 3 spectra, and Fig. 5(e) shows the particle centers determined by local maxima in the MCARS spectra. Spectral classifications lasting longer than 3 spectra are caused by the asynchronous nature of the data collection, which allows closely spaced particles to blend with each other. Triggering data collection off of elastic scatter, possibly from a fast photodiode, could improve spectral collection reliability, accuracy, and intensity. Additionally, particle spectra lasting less than 3 spectra can be caused by imperfect hydrodynamic herding in which the particle did not travel maximally through the focal volume.

#### 4. Discussion

Multiplex coherent anti-Stokes Raman scattering (MCARS) based flow cytometry provides a chemically sensitive platform for sample population analysis that has the potential to work in tandem with or to replace aspects of fluorescence-based flow cytometry. Currently, the speed and configuration of our system seem to beg the question as to the feasibility of adding MCARS technology to flow cytometry (macro- or microfluidic systems). Fortunately, the performance limitations of our system are not the limitations of the technology, and MCARS could be on-track as a real addition to flow cytometers.

In the traditional (microscopy) implementation of CARS, relatively narrow-band lasers are used to excite individual Raman transitions and the emitted anti-Stokes photons are detected with a single channel detector such as a photomultiplier tube (PMT) or an avalanche photodiode (APD). These detectors can be sensitive even at very short integration times and have allowed CARS to become a viable real-time microscopy technique [17]. When applied to flow cytometry, however, this technique is limited to targeting single known Raman transitions of interest as it would be impractical to sweep the laser wavelength to cover a relatively large spectral range. Multiplex CARS (MCARS), on the other hand, circumvents this problem by exciting multiple Raman transitions simultaneously and detecting the anti-Stokes photons with a broadband detector—typically a cooled CCD-equipped spectrometer. Unfortunately, these cooled CCD detectors are slow in comparison with PMT's and APD's at up to a few hundred spectra per second. Although these cameras are relatively slow due to circuitry timings and data transfer rates, they are far from their sensitivity limits. Figure 6 shows the simulated SNR capabilities and possibilities of several commercially available CCD spectroscopic cameras and of a generic PMT (Table 1 gives the CCD specifications used for the simulations) for a photon flux of  $2.5 \times 10^6$  photons/sec/wavelength channel. This photon flux approximates the anti-Stokes photons produced above the nonresonant background in Fig. 5(a); thus, it represents a realistic value for MCARS. For biological samples, this value could improve or decrease by over 10 dB depending on system optimization and particular molecular cross-sections. Changes to the system architecture, such as using a picosecond pump laser (assuming the Stokes source remained the same) would have the triple benefit of improved spectral resolution, improved CARS generation due to increased spectral energy density, and reduced nonresonant background as it decreases quadratically with pulse temporal width [37]. Note that the values used in this simulation are not optimized; rather we used the published typical values [38–40]. The generic PMT represents performance metrics of commercially available PMTs often used in CARS microscopy. It has a simulated gain of  $10^6$ , an anode radiate sensitivity of  $8 \times 10^4$ , a noise figure (F) of 1.3, and an anode dark current of 1 nA.

Table 1. Specifications used to simulate SNR versus integration time of various CCD detectors (see Fig. 6): Newport InstaSpec X (low- and high-speed ADC settings) (Newport Stratford, Inc., Stratford, CT), Andor DU970N-BV (Andor Technology plc, Belfast, Ireland), Princeton Instruments PIXIS:100F (Princeton Instruments, Trenton, NJ). These performance specifications are typical numbers and do not necessarily represent optimized settings, but rather typical values [38–40].

	InstaSpec, Slow	InstaSpec, Fast	Andor	PI/Acton
Binned Pixels	256	256	200	100
Readout Speed	100 kHz	2 MHz	2.5 MHz	2 MHz
Dark Current (e/p/s)	0.001	0.001	0.006	0.002
Read Noise (e/p/s)	6	24	8	12
Spectral Rate (/sec)	35	185	602	450

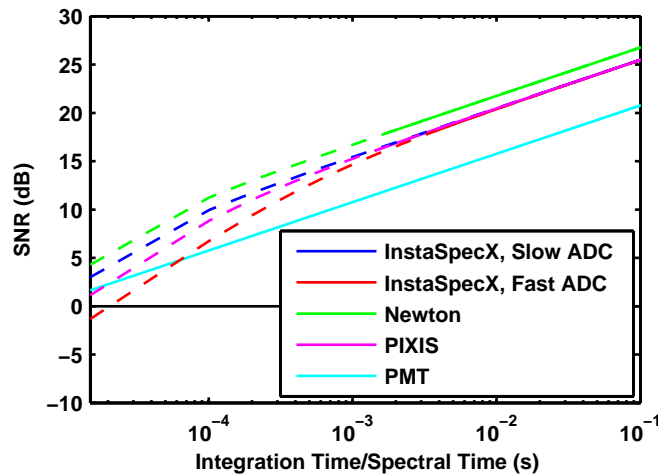


Fig. 6. (Color online) SNR of a variety of detectors: Newport InstaSpec X (low- and high-speed ADC settings), Andor DU970N-BV, PI/Acton PIXIS:100F, and a generic PMT. The solid-line portion of each plot represents currently available speeds. The dashed-portion of each plot is the calculated SNR if there were no hardware restrictions on the integration time. The black horizontal line denotes where SNR = 0 dB.

As can be deduced from Fig. 6, CCD detectors as used for MCARS are far from their speed limits. All of the CCDs simulated maintain an SNR above the generic PMT until around 10,000 spectra per second. Currently, commercially available CCDs with this level of sensitivity operate at below 1500 spectra per second (most between 15 and 200 spectra per second), but less-sensitive CCD cameras are available from 1000 frames per second to over 4,000,000 [41–43]. With high-speed technology applied to ultra-sensitive CCDs, MCARS could operate at speeds comparable and compatible with current flow cytometers. Additionally, using single-channel (or few-channel) detectors to measure elastic scatter for morphological and sizing information relaxes the speed requirements on the CCD camera. We are currently evaluating this decoupling of morphological and molecular information by integrating a separate detector for elastic scatter measurements.

## 5. Conclusion

In this work, we presented our MCARS microfluidic flow cytometer and demonstrated its ability to distinguish optically similar samples based solely on molecular composition. Furthermore, we examined the feasibility of a high-throughput system able to characterize thousands of samples per second based on the SNR provided by current MCARS systems and detector sensitivities. With the expansion of flow cytometer systems to more and more colors and without many of the technical challenges of fluorescent labels, MCARS could provide an additional layer of information to flow cytometry and even stand to replace some necessity of fluorescent labels. Compared to traditional CARS implementations, MCARS excites multiple Raman vibrations simultaneously; thus, extending CARS from vibrationally selective to molecularly sensitive, which is practically necessary when applied to flow cytometry where the sample is in constant motion. Also, as compared to traditional Raman spectroscopy, MCARS is a coherent process and therefore orders of magnitude stronger; thus, reducing detection times to the order necessary for a high-speed cytometer.

## **Acknowledgements**

This work was supported by the David and Lucile Packard Foundation.